Effective charge-spin models for quantum dots

John H. Jefferson

Defence Research Agency, Electronics Sector, St. Andrews Road, Malvern, Worcestershire WR14 3PS, United Kingdom

Wolfgang Häusler

I. Institut für Theoretische Physik, Jungiusstrasse 9, 20355 Hamburg, Federal Republic of Germany

It is shown that at low densities, quantum dots with few electrons may be mapped onto effective charge-spin models for the low-energy eigenstates. This is justified by defining a lattice model based on a many-electron pocket-state basis in which electrons are localized near their classical ground-state positions. The equivalence to a single-band Hubbard model is then established leading to a charge-spin ($t-J-V$) model which for most geometries reduces to a spin (Heisenberg) model. The method is refined to include processes which involve cyclic rotations of a ''ring'' of neighboring electrons. This is achieved by introducing intermediate lattice points and the importance of ring processes relative to pair-exchange processes is investigated using high-order degenerate perturbation theory and the WKB approximation. The energy spectra are computed from the effective models for specific cases and compared with exact results and other approximation methods. [S0163-1829(96)03731-9]

I. INTRODUCTION

Technological advances in microfabrication with corresponding reduction in feature sizes has led to renewed interest in the transport properties of semiconductor submicrometer structures both from the fundamental physics point of view and for possible future applications. In small metallic islands the Coulomb blockade gives rise to the single-electron effects, which may be modeled classically by a small intradot capacitance.[1] Islands fabricated on the basis of semiconductors, called quantum dots, show in addition to the charging effects discrete energy levels related to size quantization.[2–4] Individual quantum dots may be fabricated from heterostructures, which limits the electron motion to two dimensions, by imposing lateral confinement with a metallic gate electrode deposited using fine-line (e-beam) lithography.[4] The discrete energy spectra may be measured in transport experiments at finite voltages[5,6] or frequencies.[7] The influence of Coulomb correlations on the excitation energies is difficult to see optically by far infrared absorption[8] due to the generalized version of Kohn's theorem.[9] The observation of the quadrupole transitions by using grating couplers has been suggested[10] as a possible optical means.

Quantum dots have been referred to as ''artificial atoms''[11] since the number of conducting electrons can be smaller than 10 or 20. At the low electron densities which are experimentally accessible, the calculation of excitation energies becomes a challenging theoretical problem. For real atoms, an independent-electron picture correctly describes the main physics and the Hartree-Fock approximation yields reasonably accurate eigenstates which may be refined in a controlled way by perturbation theory. This is not generally the case for semiconducting quantum dots for which even an optimal Hartree-Fock approximation is significantly in error[12] and can even give qualitatively incorrect results, such as the wrong spin-multiplet structure. The reason for this qualitatively different behavior is that the electrons in a semiconducting quantum dot are highly correlated, due to the low effective density and the restriction of the electron motion to only two dimensions. Many-body effects must be taken into account. This has been done by numerically exact diagonalizations for systems with a very few electrons ($N \leq 4$).[13] In order to obtain reasonably accurate spectra for systems with more electrons, approximations must be made. One technique which has achieved some measure of success at low electron densities is based on many-electron ''pocket'' states.[14] Low-energy spectra of systems with up to six electrons have been determined accurately[15] and the agreement with the exact numerical solutions ($N \leq 4$) is good. Unfortunately the computational effort is likely to become prohibitive for systems with more than ten electrons and we are again faced with the problem of devising a reliable approximation method for such cases.

One possible route is suggested by the pocket-state analysis itself, which exploits the permutation symmetry of the wave functions. We notice that in many cases the eigensolutions may be represented by an effective spin model of a simple form (Heisenberg model). This apparent equivalence is reminiscent of magnetic insulators for which the correlated electron problem is known to reduce to a spin Hamiltonian, a mapping which may be justified by transformation theory[16] or degenerate perturbation theory[17] as well as, in some cases, by the theory of permutation groups.[18] The magnetic insulator problem starts with a lattice model in which the electrons are localized on atomiclike orbitals and for which electron correlations are essential, the generic model being the so-called Hubbard model.[19] The underlying crystalline lattice establishes sites on which suitable one-electron states are centered. The question arises as to what circumstances, if any, might a Hubbard-type model be applicable to the problem of interacting electrons in a quantum dot, for which the Fermi wavelengths are much larger than the interatomic spacings and the underlying crystalline lattice loses its significance. At extremely low electron densities the long-range

interaction energy, according to Wigner,[20] creates a crystal-linelike ground state which might define new electronic lattice sites. This crystallization is expected to take place only at electron densities which are a factor of 20 smaller than the densities used in experiments. Nevertheless, it has been shown that the assumption of localized electrons allows the calculation of discrete low-energy excitations as quantum corrections to the Wigner crystal energies.[15] The validity of a Hubbard model description is not only an interesting question of principle but has the practical potential of enabling systems of many more electrons to be dealt with than has hitherto been the case, i.e., tens of electrons or more. This would enable the full machinery of techniques for solving the Hubbard and Heisenberg models to be applied, for which there has been much progress in recent years following the discovery of high-temperature superconductivity and the associated theoretical activity on correlated electron systems.[21]

In this paper we will show that such a mapping may indeed be justified for the *a priori* continuous problem of interacting electrons in a quantum dot at low densities. This is done through the use of pocket states which are briefly reviewed in the next section after introducing the basic interacting electron model. In Sec. III we show how the pocket states may be used to define a one-electron orthonormal basis with orbitals localized on a ''lattice,'' related to the electron configuration(s) in the classical ground state (determined by electrostatics). This is then used to construct a tight-binding Hamiltonian which reduces to the Hubbard model at low electron densities. Further mapping to an effective (Heisenberg) spin Hamiltonian or charge-spin ($t-J-V$) model is then performed.

In Sec. IV we point out an essential difference between quantum dots and the corresponding correlated electron problem for interacting electrons on a true lattice of atoms, namely, the increased importance of the so-called ''ring'' terms in the former case, which involve cyclic permutations of more than two electrons. The simple Hubbard model on a lattice underestimates the magnitude of these ring terms for the dot and it is shown how the method may be refined by introducing intermediate lattice points which are unoccupied in the ground manifold but give rise to the required ring processes through virtual excitations. In Sec. V we solve the effective Hamiltonians for specific examples with $N \leq 6$ and compare with exact numerical and pocket-state results where appropriate. Finally, in Sec. VI, we give a summary and discuss the outlook for this approach in dealing with systems of more electrons and of obtaining further corrections where necessary.

II. THE MODEL AND POCKET-STATE BASIS

We consider the N-electron quantum dot described by the Hamiltonian

$$H = \sum_{i=1}^{N} \left(\frac{\mathbf{p}_i^2}{2m} + v(\mathbf{x}_i) \right) + W(\mathbf{x}_1, \ldots, \mathbf{x}_N),$$

$$W(\mathbf{x}_1, \ldots, \mathbf{x}_N) = \frac{1}{2} \sum_{\substack{i,j \\ i \neq j}} w(|\mathbf{x}_i - \mathbf{x}_j|), \qquad (2.1)$$

where $\mathbf{x}_i$ and $\mathbf{p}_i$ are position and momentum of the ith electron in d dimensions ($d=2$ for most quantum dots) with (effective) mass m and spin $s=1/2$. Neither the one-particle confinement potential $v(\mathbf{x})$ nor the interaction $w(x)$ depend explicitly on spin.

The cases of square well single-particle potentials in one dimension (1D) and in two dimensions (for square geometry) have been discussed in Ref. 15. To be specific, and for comparison later, we shall also mainly confine ourselves to the 2D square potential well of square geometry, though the extension to other geometries is straightforward and, for the present consideration, the detailed form of $v(\mathbf{x})$ is not qualitatively important. At large mean interparticle distances r_s it becomes energetically favorable for the electron system to localize its charge density distribution in regions close to the classical ground-state electron configuration(s),[20,22] which may be determined by minimizing the electrostatic energy.

This fact is the motivation for the many-electron pocket-state basis in which the Hilbert space is restricted to $1 \leq p \leq \nu N!$ basis states $|p\rangle$ with spatial representations being defined in configuration space of dimensionality dN. The number of classical minimum-energy configurations ν may be greater than one in certain symmetric geometries. (For example, for $N=3$ on a square we have $\nu=4$ since, for the classical ground-state energy, any one of the four corners may be unoccupied.) The low-energy levels form a multiplet which contains $\nu 2^N$ states in total (including Zeeman levels). The excited ''vibrational'' states scale as a power law $\sim r_s^{-\gamma}$ with r_s (γ being close to 3/2) and can be neglected if the density is not too high. This is due to the scaling $\sim \exp(-\sqrt{r_s/r_c})$ of the low-energy excitations we are interested in here, where r_c is a length scale which characterizes the transition from the almost noninteracting situation ($r_s \ll r_c$) into the qualitatively different regime of strong correlations ($r_s \gg r_c$).[14]

In the pocket-state method, the first step is to calculate energies by assuming equivalent but distinguishable particles and ignoring their spin. Spin and statistics are subsequently reestablished by means of group theory. Tunneling integrals $\langle p|H|p'\rangle$ between the localized many-particle (pocket) basis states determine the low-energy excitations. The tunneling processes correspond to (correlated) transitions between different particle arrangements. In the low-density regime one tunneling integral, $J/2$, is exponentially larger than all others. In many cases the dominant J corresponds to the exchange of only two particles, which may be adjacent in real space. Other processes could be the simultaneous (ring) exchange of three or more particles, corresponding to a cyclic permutation.

An important feature of the spectra given by the pocket-state approximation (and by the effective charge-spin models to be derived and discussed in the following sections) is that the fine structure of the energy spectra depends only on J, the magnitude of which may be estimated semiclassically within the multidimensional WKB approximation. The ratios between the energy differences are insensitive to the detailed form of the interelectron potential and to r_s. An examination of the spectra shows that these situations may be mapped onto an effective spin model with again one parameter for each process (pair exchange, ring) considered. This equivalence will be justified in the next section. Here we merely

make the observation that for the cases considered by the pocket-state method, the energy spectrum is the same as that which would be given by a spin Hamiltonian. An exception to this are situations for which more than one classical minimum-energy configuration for the electrons exist ($\nu > 1$), such as two or three electrons on a square. We will show in the next section that these latter situations may be mapped onto a so-called $t - J - V$ model in which the dominant tunneling process is now related to t, the amplitude corresponding to the jump of a single particle into an empty ''site.'' J is again an exchange process involving at least two particles and V represents the Coulomb repulsion between electrons on neighboring ''sites.''

In general, the pocket states are correlated electron states which need not be assumed as a direct product of one-electron states. However, we may mimic the eigenstates at sufficiently large r_s with a one-electron product basis within the Heitler-London (HL) approximation. The latter are localized in regions close to the positions the electrons would have in the classical ground state. In the next section we show how this one-electron basis may be used to define an orthonormal basis from which we construct an effective Hubbard model. This effective Hamiltonian yields low-energy spectra which are at least as accurate as what would be given by the corresponding HL approximation using a product basis of nonorthogonal, one-electron wave functions. We then show in Sec. IV how the method may be extended to cases where ring processes are important.

III. MAPPING TO HUBBARD AND CHARGE-SPIN MODELS

Let us assume that the pocket basis states $|p\rangle$ are approximated ''optimally'' by nonorthogonal one-electron wave functions ϕ_i centered at position i. These states have the form

$$\langle \mathbf{x}_1, \ldots, \mathbf{x}_N | p \rangle \equiv \phi_{p_1}(\mathbf{x}_1) \phi_{p_2}(\mathbf{x}_2) \cdots \phi_{p_N}(\mathbf{x}_N), \qquad (3.1)$$

where $\{p_1, \ldots, p_N\}$ is the permutation p of the sequence $\{1, \ldots, N\}$. In this section we orthogonalize these one-electron wave functions and construct antisymmetrized N-electron states from which we define the effective Hubbard model, which is subsequently transformed into a spin Hamiltonian. To illustrate the main features of the method with minimal mathematical complexity, we first consider in detail the simplest nontrivial case of two electrons in a 1D square well. The analysis is then generalized to N electrons in one or two dimensions.

As is well known, for two electrons the antisymmetrized states may be written as the product of orbital and spin parts, as with the HL states of the hydrogen molecule. The symmetric (singlet) and antisymmetric (triplet) orbital states are thus

$$\Psi_S = \frac{\phi_1(1)\phi_2(2) + \phi_2(1)\phi_1(2)}{\sqrt{2(1+s^2)}} \qquad (3.2)$$

and

$$\Psi_A = \frac{\phi_1(1)\phi_2(2) - \phi_2(1)\phi_1(2)}{\sqrt{2(1-s^2)}}, \qquad (3.3)$$

where $s = \langle \phi_1 | \phi_2 \rangle$ is the overlap and the arguments $(i=1,2)$ abbreviate the coordinate $\mathbf{x}_i$ of the ith particle. These HL states yield approximate singlet and triplet ground-state energies: $E_{\text{singlet}} = \langle \Psi_S | H | \Psi_S \rangle$ and $E_{\text{triplet}} = \langle \Psi_A | H | \Psi_A \rangle$, where H is the Hamiltonian for two electrons given by Eq. (2.1).

We now transform to orthonormal one-electron states ψ where

$$\psi_1 = \left(\frac{1}{2\sqrt{1+s}} + \frac{1}{2\sqrt{1-s}} \right) \phi_1 + \left(\frac{1}{2\sqrt{1+s}} - \frac{1}{2\sqrt{1-s}} \right) \phi_2,$$

$$\psi_2 = \left(\frac{1}{2\sqrt{1+s}} + \frac{1}{2\sqrt{1-s}} \right) \phi_2 + \left(\frac{1}{2\sqrt{1+s}} - \frac{1}{2\sqrt{1-s}} \right) \phi_1. \qquad (3.4)$$

Inverting this transformation and substituting into Eqs. (3.2) and (3.3) we get

$$\Psi_S = \frac{1}{\sqrt{1+s^2}} \Psi_S^{(1)} + \frac{s}{\sqrt{1+s^2}} \Psi_S^{(2)}, \qquad (3.5)$$

$$\Psi_S^{(1)} = \frac{\psi_1(1)\psi_2(2) + \psi_2(1)\psi_1(2)}{\sqrt{2}},$$

$$\Psi_S^{(2)} = \frac{\psi_1(1)\psi_1(2) + \psi_2(1)\psi_2(2)}{\sqrt{2}}, \qquad (3.6)$$

and

$$\Psi_A = \frac{\psi_1(1)\psi_2(2) - \psi_2(1)\psi_1(2)}{\sqrt{2}}. \qquad (3.7)$$

We note that Ψ_A (triplet) has the same form as for the nonorthogonal states given in Eq. (3.3), i.e. it corresponds to one electron in each orbital. On the other hand, Ψ_S (singlet) consists of two components, one with an electron on each orbital ($\Psi_S^{(1)}$) and the other with both electrons in the same orbital ($\Psi_S^{(2)}$). (The latter state is not allowed for the triplet by the Pauli principle.) This ''double occupation'' is thus a direct consequence of orthogonalization.

Using these two-electron states composed of orthogonal one-electron wave functions will, of course, yield exactly the same approximate singlet and triplet energy expectation values. However, we can obtain a more accurate estimate for the ground-state energy of the singlet by diagonalizing the Hamiltonian in the Hilbert space defined by the two-electron base states $\Psi_S^{(1)}$ and $\Psi_S^{(2)}$ [Eq. (3.6)]. This follows from the variational principle which ensures that diagonalization of the Hamiltonian matrix will yield the optimum superposition of the base states, whereas the HL state (3.5) is not optimum in general.

This principle also applies to the general N-electron case as stated in the Introduction, i.e., diagonalization of the Hamiltonian in the restricted Hilbert space defined by base states (Slater determinants) constructed from orthogonalized one-electron wave functions will yield a more accurate low-

energy spectrum than the simple products of nonorthogonal one-electron states (3.2) and (3.3).

For the two-electron case the (2×2) Hamiltonian singlet matrix is

$$H_s = \begin{pmatrix} 2\varepsilon + V + j & 2\widetilde{t} \\ 2\widetilde{t}^* & 2\varepsilon + U + \widetilde{j} \end{pmatrix}, \qquad (3.8)$$

where

$$\varepsilon = \left\langle \psi_1 \left\| \left[\frac{\mathbf{p}^2}{2m} + v \right] \right\| \psi_1 \right\rangle = \left\langle \psi_2 \left\| \left[\frac{\mathbf{p}^2}{2m} + v \right] \right\| \psi_2 \right\rangle,$$

$$V = \int |\psi_1(\mathbf{x})|^2 |\psi_2(\mathbf{y})|^2 w(|\mathbf{x} - \mathbf{y}|) d^3x \; d^3y,$$

$$U = \int |\psi_1(\mathbf{x})|^2 |\psi_1(\mathbf{y})|^2 w(|\mathbf{x} - \mathbf{y}|) d^3x \; d^3y$$

$$= \int |\psi_2(\mathbf{x})|^2 |\psi_2(\mathbf{y})|^2 w(|\mathbf{x} - \mathbf{y}|) d^3x \; d^3y,$$

$$t = \int \psi_1^*(\mathbf{x}) \left[\frac{\mathbf{p}^2}{2m} + v(\mathbf{x}) \right] \psi_2(\mathbf{x}) d^3x,$$

$$\tau = \int \psi_1^*(\mathbf{x}) \left[\int |\psi_1(\mathbf{y})|^2 w(|\mathbf{x} - \mathbf{y}|) d^3y \right] \psi_2(\mathbf{x}) d^3x,$$

$$\widetilde{t} = t + \tau,$$

$$j = \int \psi_1^*(\mathbf{x}) \psi_2^*(\mathbf{y}) w(|\mathbf{x} - \mathbf{y}|) \psi_2(\mathbf{x}) \psi_1(\mathbf{y}) d^3x \; d^3y,$$

$$\xi = \int \psi_2^*(\mathbf{x}) \psi_2^*(\mathbf{y}) w(|\mathbf{x} - \mathbf{y}|) \psi_1(\mathbf{x}) \psi_1(\mathbf{y}) d^3x \; d^3y,$$

$$\widetilde{j} = \mathrm{Re}(\xi). \qquad (3.9)$$

Note, $j = \xi = \widetilde{j}$ if the ψ_i are real.

The triplet energy is

$$E_t = 2\varepsilon + V. \qquad (3.10)$$

Within this restricted manifold of states, the singlet-triplet Hamiltonian matrix, Eqs. (3.8) and (3.10), are equivalent to an effective Hamiltonian,

$$H_{\mathrm{eff}} = \varepsilon[n_1 + n_2] + U[n_{1\uparrow} n_{1\downarrow} + n_{2\uparrow} n_{2\downarrow}] + V n_1 n_2$$

$$+ j \sum_\sigma c_{1\sigma}^\dagger c_{2\overline{\sigma}}^\dagger c_{2\sigma} c_{1\overline{\sigma}} + \left[\sum_\sigma \left(t c_{1\sigma}^\dagger c_{2\sigma} + \tau(c_{1\sigma}^\dagger c_{2\sigma} n_{1\overline{\sigma}} \right. \right.$$

$$\left. \left. + c_{2\sigma}^\dagger c_{1\sigma} n_{2\overline{\sigma}}) + \frac{1}{2} \xi c_{1\sigma}^\dagger c_{1\overline{\sigma}}^\dagger c_{2\overline{\sigma}} c_{2\sigma} \right) + \mathrm{H.c.} \right], \qquad (3.11)$$

where $c_{i\sigma}^\dagger$ is a Fermi creation operator at site $i = 1, 2$ satisfying $\langle \mathbf{x} | c_{i\sigma}^\dagger | \mathrm{vac} \rangle = \psi_{i\sigma}(\mathbf{x})$; $n_{i\sigma} = c_{i\sigma}^\dagger c_{i\sigma}$ and $n_i = n_{i\uparrow} + n_{i\downarrow}$.

This effective Hamiltonian is very similar to that considered by Hubbard[19] for a periodic array of one-electron atoms in the study of the metal-insulator (Mott) transition. Indeed, for this two-electron case, Eq. (3.11) is an effective Hamiltonian for the hydrogen molecule within a restricted Hilbert space of (effective) $1s$ orbitals. We stress, however, that in the quantum dot case the localized orbitals are fundamentally different from those in the atomic case in that their very existence depends on the electron-electron repulsion which is responsible for localizing the electrons near specific points in real space at low density. For this reason we are not justified, *a priori*, in dropping all but the largest Coulomb term (U), as is usually done in the Hubbard model. In particular, the nearest-neighbor effective Coulomb interaction V becomes most important when r_s becomes very large and Eq. (3.11) simply reduces to the classical expression for the ground-state energy, independent of spin, as it should. This may be seen more clearly by transforming (3.11) into an effective spin Hamiltonian which is demonstrated most directly for this two-electron case by diagonalizing the singlet matrix, (3.8), explicitly to yield eigenenergies

$$E_\pm = \frac{1}{2} \left[4\varepsilon + V + U + j + \widetilde{j} \pm \sqrt{(U - V + \widetilde{j} - j)^2 + 16|\widetilde{t}|^2} \right]. \qquad (3.12)$$

Since for the cases of interest (large separation between the electrons and real one-particle wave functions), $U \gg V, j, \widetilde{j}$ and $j = \widetilde{j}$, then

$$E_+ \approx 2\varepsilon + U + j + \frac{4|\widetilde{t}|^2}{U - V} \qquad (3.13)$$

and

$$E_- \approx 2\varepsilon + V + j - \frac{4|\widetilde{t}|^2}{U - V}. \qquad (3.14)$$

Combining these equations with (3.10) for the triplet we see that the energy spectrum consists of a singlet-triplet pair at low energies separated by a singlet at energy $\sim U$ higher. Hence the low-energy singlet triplet is equivalent to a spin system with effective spin Hamiltonian

$$H_{\mathrm{spin}} = 2\varepsilon + V + J(\mathbf{s}_1 \cdot \mathbf{s}_2 - 1/4), \qquad (3.15)$$

where

$$J = \frac{4|\widetilde{t}|^2}{U - V} - j \approx \frac{4|\widetilde{t}|^2}{U} - j. \qquad (3.16)$$

The first term in Eq. (3.16), favoring a singlet ground state, is sometimes referred to as "superexchange" and is usually larger than the second "direct" exchange term, j. This superexchange contribution has its origins in the assumed nonorthogonality of the initial Heitler-London basis ϕ_i in (3.1). From the pocket states it is known that they form a nonorthogonal basis set for the low-energy eigenstates.[23]

We now consider the general case of N electrons in a quantum dot. Starting with a suitable product basis of pocket states, Eq. (3.1), we may, in general, define an orthonormal basis by Löwdin's method.[24] [For high-symmetry situations it may be more convenient and expedient to use some other method. For example, in the case of four electrons on a square we have $\pi/4$ rotational symmetry and we may generate orthonormal states by forming molecular orbitals, normalizing, and then transforming back to localized states. Similarly, for translationally invariant systems we may transform to running (Bloch) waves, normalize, and then trans-

form back to localized (Wannier) states.] Within the corresponding many-electron Hilbert space we may express the Hamiltonian in second quantized form. We are led directly to an effective ''single-band'' model of the type considered by Hubbard, generalizing Eq. (3.11),

$$H_{\text{eff}} = \sum_i \left[\varepsilon_i n_i + U_i n_{i\uparrow} n_{i\downarrow} \right] + \sum_{i,j} V_{ij} n_i n_j$$

$$+ \sum_{ij\sigma} j_{ij} c_{i\sigma}^\dagger c_{j\bar\sigma}^\dagger c_{j\sigma} c_{i\bar\sigma} + \left[\sum_{i,j,\sigma} \left(t_{ij} c_{i\sigma}^\dagger c_{j\sigma} \right. \right.$$

$$+ \tau_{ij} (c_{i\sigma}^\dagger c_{j\sigma} n_{i\bar\sigma} + c_{j\sigma}^\dagger c_{i\sigma} n_{j\bar\sigma})$$

$$\left. \left. + \frac{1}{2} \xi_{ij} c_{i\sigma}^\dagger c_{i\bar\sigma}^\dagger c_{j\bar\sigma} c_{j\sigma} \right) + \text{H.c.} \right], \quad (3.17)$$

where the indices i and j should be distinct. The parameters ε, U, V, j, t, τ, and ξ have the same meaning as in the two-electron case (3.9), though it should be noted that they will, in general, depend on the position of the electron, or pair of electrons and on separation. In particular the parameters, j, t, τ, and ξ related to electron transfers decay rapidly as the distance between the sites i and j increases. This allows us to retain only nearest-neighbor terms in the double summations. As with the case of two electrons, we may eliminate the high-energy states of H_{eff} to yield an effective spin Hamiltonian. This may be done using degenerate perturbation theory[25] or a canonical transformation,[26] as with the case of a lattice.

Specifically in the situations of two- (or higher-) dimensional quantum dots the cases of more than one minimum of the classical electrostatic energy may occur ($\nu > 1$). Then the quantum-mechanical charge density distribution shows more than N peaks at large r_s, say $\widetilde{N} > N$. The number of single-electron states must be equal to $\widetilde{N}$ in these cases. $\widetilde{N} - N$ lattice sites will be unoccupied at an instant. Consider, for example, the case of a square confining potential in two dimensions. For $N = 2$, $\widetilde{N} = 4$ and the electrons will be found mainly near opposite vertices along the diagonal of the square, due to the Coulomb repulsion. States with two electrons near adjacent vertices will be of order V higher in energy (nearest-neighbor Coulomb repulsion energy) and states with two electrons located near the same vertex will be of order U higher in energy. Similarly for $N = 3$ there will be low-lying states with electrons located near three of the $\widetilde{N} = 4$ vertices with states having two electrons near the same vertex again being $\sim U$ higher in energy. For $N = 4$ all vertices are occupied in the ground manifold, with configurations for which there are two electrons near one vertex being at least $\sim U$ higher in energy.

In each of these cases the high-energy states, corresponding to one or more vertices being occupied by two electrons, may be eliminated from the Hilbert space by degenerate perturbation theory, where they appear as intermediate states. More precisely, we first write H_{eff} in the form $H_{\text{eff}} = H_0 + H_1$ where $H_0 = \sum_i [\varepsilon_i n_i + U_i n_{i\uparrow} n_{i\downarrow}]$. H_0 is diagonal in the basis of product states with the highest-energy states having two electrons in the same state, being $\sim U$ higher than the low-energy states.[27] Eliminating these states to second-order results in an effective ''$t - J - V$'' Hamiltonian,[28]

$$H_{\text{eff}}^{tJV} = P \sum_{i,j} \left[\sum_\sigma (t_{ij} c_{i\sigma}^\dagger c_{j\sigma} + \text{H.c.}) \right.$$

$$\left. + J_{ij} (\mathbf{s}_i \cdot \mathbf{s}_j - 1/4) n_i n_j + V_{ij} n_i n_j \right] P. \quad (3.18)$$

In this equation t and V have the same meaning as before and

$$J_{ij} = 2|t_{ij} + \tau_{ij}|^2 \left[\frac{1}{U_i} + \frac{1}{U_j} \right] - j_{ij}. \quad (3.19)$$

P is a projection operator which eliminates all base states for which there are two electrons in the same localized state. [These states appear as intermediate states and give rise to the superexchange in Eq. (3.19).] We also note that the ε, τ, and ξ terms in Eq. (3.17) have disappeared in Eq. (3.18). The former has been dropped since it always gives rise to a constant and the latter two are precluded by P (as is the U term) since they would always give rise to double occupation at a site.

Equations (3.17) and (3.18) are the fundamental effective Hamiltonians for interacting electrons at low density in a quantum dot and capture the main physics of the problem for most situations. (They do not, however, include processes in which groups of electrons can rotate simultaneously, which can be important in some circumstances. The generalization to include these so-called ring terms is given in the next section.) Although these effective models were justified by starting with the Heitler-London approximation to pocket states using nonorthogonal one-electron states, we emphasize that they have a greater range of validity than the initial approximation suggests. The above methodology enabled us to define a basis set of product states (Slater determinants) of some one-electron states and this led directly to effective Hamiltonians operating within this restricted (incomplete) basis set. However, it is well known[25] that higher-lying base states may be accounted for by perturbation theory. This technique has recently been applied very successfully to lattice models in which an effective single-band Hubbard model was derived from a multiband model using quaside-generate perturbation theory.[29] We shall not attempt such a reduction here for the quantum dot problem, but merely point out that its main effect would be to renormalize the effective parameters ($\varepsilon_i, U_i, t_{ij}$, etc.) and extend the validity of the resulting models.

Let us apply (3.18) to the case of electrons in a square well in two dimensions, discussed above. For $N = 2$ and $N = 3$ the t term will cause electrons to hop from occupied to unoccupied sites whereas the J and V terms will be effective only when two adjacent sites are occupied. The presence of the V term ensures that for $N = 2$ the electrons will have lower energy when they are located on diagonally opposite vertices of the well, as mentioned earlier. For $N = 4$ the t term may be omitted since all four vertices are occupied in the ground manifold and it would thus give rise to double occupancy, precluded by P. The V term may also be dropped since it gives rise to a constant contribution. Hence the sites i and j can be restricted to nearest neighbors so that (3.18) reduces to a Heisenberg model,
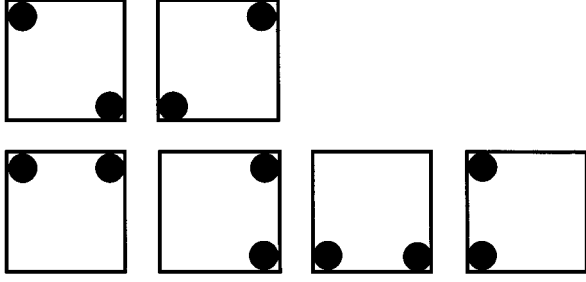
FIG. 1. Classical low-energy configurations for two electrons in a 2D square quantum well. The first two configurations are lowest in energy while the remaining four are V higher in energy due to Coulomb repulsion. All other configurations have higher electrostatic energy.

$$H_J = \sum_{\langle i,j \rangle} J_{ij} \mathbf{s}_i \cdot \mathbf{s}_j, \tag{3.20}$$

where P has been omitted for brevity.

Similar considerations apply for $N > 4$ and the effective Hamiltonian will either have the form (3.20) or (3.18), depending on whether $\nu = 1$ (e.g., $N = 4,5$) or $\nu > 1$ (e.g., $N = 2,3,6$). For the latter cases a further reduction will be possible when some of the states of the $t-J-V$ model are clearly higher in energy due to the V interaction.

Consider, for example, the case of two electrons in a square-shaped dot for which there are six ways of distributing the two (indistinguishable) electrons in the four corners, resulting in a Hilbert space of dimension $4 \times 6 = 24$ when spin is taken into account. Four of these configurations (16 with spin) are of order V higher in energy than the remaining two, as shown in Fig. 1. These high-energy base states may be eliminated from the problem by a further application of degenerate perturbation theory, resulting in an effective Hamiltonian which only operates in the Hilbert space of the eight lowest-energy base states. By a straightforward calculation this takes the form (apart from an unimportant overall constant)

$$H_{\text{eff}} = \Delta (n_1 n_3 - n_2 n_4)(R_{\pi/2} - R_{-\pi/2}) + J[(\mathbf{s}_1 \cdot \mathbf{s}_3 - 1/4)n_1 n_3$$
$$+ (\mathbf{s}_2 \cdot \mathbf{s}_4 - 1/4)n_2 n_4], \tag{3.21}$$

where $\Delta = 2t^2/V$ and R_θ is a rotation operator, i.e.,

$$R_{\pi/2}|\sigma, *, \sigma', *\rangle = |*, \sigma, *, \sigma'\rangle, \tag{3.22}$$

etc. Note that the prefactor $(n_1 n_3 - n_2 n_4)$ takes the value ± 1 depending on whether either sites 1 and 3, or 2 and 4 are occupied. This effective Hamiltonian is easily diagonalized. The spectrum consists of two singlets and two triplets. We see immediately that (3.21) gives zero when operating on a spin-polarized state and hence the triplets are at zero energy with the singlets at energies $-J \pm 2\Delta$, in agreement with what is obtained from the pocket-state approximation for this problem when the exchange of the two electrons is included there.[15] There are thus two contributions to the "binding energy" of the singlet ground state, a resonance energy (-2Δ) and a superexchange energy $(-J)$. It is easy to see that the former will be dominant since it occurs in second

order and does not involve double occupation of a site. On the other hand, there are two contributions to J, the second-order term $\sim 4t_{13}^2/U$ and fourth-order terms $\sim t_{12}^4/V^2 U$. We may extend these considerations to a regular polygon with N vertices and $N/2$ electrons. The effective Hamiltonian will again consist of rotation operators (of $\pm 2\pi/N$) and exchange terms. The exchange terms are independent of N, whereas the rotation terms become relatively less important since they first occur in Nth order. In the next section we shall encounter circumstances where simultaneous rotations of more than two electrons may be important.

We conclude this section by emphasizing the computational advantage in this reduction to a spin or charge-spin Hamiltonian. Thus, for example, the Heisenberg model lies in a Hilbert space of dimension 2^N for N electrons, which may be further reduced by exploiting other symmetries, e.g., conservation of total S_z which reduces the largest subspace to $N!/[(N/2)!]^2$ ($S_z = 0$ for N even). This should be compared with

$$\max_S \left[\frac{(2S+1)N!}{(N/2+S+1)!(N/2-S)!} \right]^2$$

for the largest subspace of the Hamiltonian in the original pocket-state basis.

The mapping also gives interesting insight into the nature of the energy spectrum. For those cases which reduce to a Heisenberg model, the spectrum consists of spin multiplets with energy separation of order J ("bandwidth" $\sim 2NJ$). On the other hand, for cases which reduce to a charge-spin model, there are multiplets separated by energies of order $t (\gg J$ in the same geometry and electron densities), each of which have a fine structure with energy splittings of order J.

The foregoing analysis for electrons may also be extended to a fictitious system of spin-1/2 charged bosons. For repulsive Coulomb interactions they also show Wigner crystallization and the pocket-state method can be applied. This problem was considered by Häusler[15] in order to prove that the state of highest spin within the multiplet structure of electrons (fermions) in a quantum dot is the spin-polarized state for $\nu = 1$ by exploiting an isomorphism between fermions and bosons using permutation group theory. We consider this problem here to enable another direct comparison with the pocket-state description.

The case of spin-1/2 bosons is similar to the fermion case in that at low densities the largest "Coulomb" matrix elements correspond to two bosons on the same site. Neglecting all other matrix elements thus gives the "boson" Hubbard model:

$$H = \sum_{\langle i,j \rangle \sigma} (t_{ij} b_{i\sigma}^\dagger b_{j\sigma} + \text{H.c.}) + \frac{U}{2} \sum_{i,\sigma,\sigma'} b_{i\sigma}^\dagger b_{i\sigma'}^\dagger b_{i\sigma'} b_{i\sigma}. \tag{3.23}$$

Using the usual commutation rules for the Bose operators yields

$$b^\dagger |n\rangle = \sqrt{n+1}|n+1\rangle,$$

$$b|n\rangle = \sqrt{n}|n-1\rangle. \tag{3.24}$$

It follows that

$$h_0|\sigma,\sigma'\rangle=U|\sigma,\sigma'\rangle,$$

where

$$h_0=\frac{U}{2}\sum_{\sigma\sigma'}b_\sigma^\dagger b_{\sigma'}^\dagger b_{\sigma'}b_\sigma.$$

This is the same result as the case of fermions except that with bosons the two particles may have the same spin.

As with the fermion case, we can now reduce (3.23) to a Heisenberg or $t-J-V$ model (depending on whether or not the number of bosons equals the number of lattice sites). Let us, for simplicity, do this for just two sites. The extension to the general case may be done by perturbation theory in the same way as with fermions.

In the "atomic limit" ($t=0$) the eigenstates of (3.23) with two bosons consist of either one boson on each site with either spin (energy 0) or one site unoccupied and the other doubly occupied, again with either spin (energy equal to U). Using these base states it is straightforward to show that the singlet state

$$|\psi_S\rangle=\frac{|\uparrow,\downarrow\rangle-|\downarrow,\uparrow\rangle}{\sqrt{2}}$$

is unaffected by the hopping, i.e.,

$$H|\psi_S\rangle=0.$$

On the other hand, the triplet states mix. For example, using (3.24), we get

$$H|\uparrow,\uparrow\rangle=t[|\cdot,\uparrow\uparrow\rangle+|\uparrow\uparrow,\cdot\rangle],$$

$$H|\uparrow\uparrow,\cdot\rangle=U|\uparrow\uparrow,\cdot\rangle+\sqrt{2}t|\uparrow,\uparrow\rangle,$$

etc. This leads directly to the triplet Hamiltonian matrix

$$\begin{bmatrix}0 & 2t\\2t & U\end{bmatrix},$$

with lowest eigenvalue

$$E=\frac{U-\sqrt{U^2+16t^2}}{2}.$$

This is exactly the same result as for the fermions except that the positions of the (lowest) singlet and triplet levels are reversed. It follows that the lowest singlet and triplet are equivalent to a Heisenberg model with ferromagnetic exchange of the same magnitude as the case of fermions. As mentioned above, this may be generalized to any number of sites by degenerate perturbation theory resulting in a Heisenberg model in which $J\rightarrow-J$ when compared with the fermion case, leading to an "inverted" spectrum in agreement with the permutation group analysis described in the second reference of Ref. 15.

In a similar fashion, cases for which the number of bosons is less than the number of sites (such as two or three on a square) may be reduced to a $t-J-V$ model. However, while the sign of J is reversed relative to the case of fermions, the sign of t remains the same and the resulting spectrum is no longer a simple inversion.
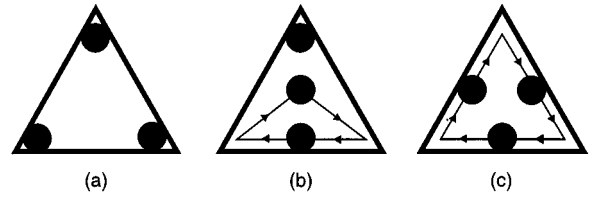

FIG. 2. (a) Classical ground-state configuration for three electrons in a triangular quantum dot. (b) Classical path for the exchange of two electrons. (c) Classical path for the cyclic permutation of all three electrons. Particles are shown in intermediate positions along their trajectories.

IV. RING TERMS

In Sec. III it was shown that the $t-J-V$ model may be reduced to an effective Hamiltonian which only involves the lowest-energy base states. This effective Hamiltonian then contains operators which rotate some or all of the electrons simultaneously [cf. (3.21)]. The possibility of such a collective motion of a subset or all of the electrons is much more general and will in fact occur for any geometry. These processes are negligible within the framework of the usual lattice models but this is not always the case in quantum dots or other semiconductor based nanostructures where such "ring" terms can become dominant. As we shall see they may be included in a lattice model by introducing intermediate lattice points which are unoccupied in the ground manifold.

Consider, for example, the case of an equilateral triangular dot containing three electrons, as shown in Fig. 2. Using the Hilbert space defined by the Heitler-London approximation to the pocket states leads directly to the Heisenberg model for this system, with a spin-1/2 ground state, as shown in Sec. III. Ring terms corresponding to cyclic rotations of all three electrons are not included in this model. However, it is clear from the pocket-state description that such processes exist. The relevant tunneling integrals between the $3!=6$ pocket states in this case can be represented by permutations of the types

$$(123)\rightarrow(213):\quad J/2\quad(\text{pair exchange}),$$

$$(123)\rightarrow(312):\quad K/2\quad(\text{ring exchange}).$$

Their magnitudes may be estimated semiclassically within the WKB approximation. The most important contributions to J and K vary exponentially with the particle distance r_s (which equals the length of one side of the triangle in the case considered), i.e.,

$$J/2\sim e^{-\mathcal{S}_{(123)\rightarrow(213)}},\quad K/2\sim e^{-\mathcal{S}_{(123)\rightarrow(312)}},$$

where

$$\mathcal{S}=\int_0^1 dq\sqrt{2mnW(\mathbf{x}(q))}$$

is the action associated with the transport of n particles ($n=2$ or $n=3$ for J or K, respectively) of mass m from the initial classical ground state (123) into the final state. The transition takes place along the trajectory $\vec{\mathbf{x}}(q)$ which in principle

obeys an equation of motion which minimizes the classical action. Here, it is parametrized by $0 \leq q \leq 1$ in configuration space (of dimensionality $dN=6$). For an explicit estimate let us specify the interaction between the particles and assume

$$w(|\mathbf{x}_i - \mathbf{x}_j|) = \frac{e^2/\kappa}{|\mathbf{x}_i - \mathbf{x}_j|}.$$

Then $W(\vec{\mathbf{x}})$ is the Coulomb energy at $\vec{\mathbf{x}} \equiv \{\mathbf{x}_1, \mathbf{x}_2, \mathbf{x}_3\}$ where the equilibrium value $3(e^2/\kappa)/r_s$ has been subtracted so that $W(\vec{\mathbf{x}}(0)) = W(\vec{\mathbf{x}}(1)) = 0$. The results

$$\mathcal{S}_{(123) \to (213)} = 4\sqrt{m\frac{e^2}{\kappa}r_s} \int_0^{1/2} dq \left[\frac{1}{\sqrt{1-q+q^2}} \right.$$

$$+ \frac{1}{\sqrt{1-\frac{29}{8}q+4q^2}}$$

$$\left. + \frac{1}{\sqrt{1-\frac{5}{2}q+\frac{7}{4}q^2}} - 3 \right]^{1/2}$$

$$= 2.139\sqrt{r_s m e^2/\kappa},$$

$$\mathcal{S}_{(123) \to (312)} = 6\sqrt{m\frac{e^2}{\kappa}r_s} \int_0^{1/2} dq \left[\frac{1}{\sqrt{1-3q+3q^2}} - 1 \right]^{1/2}$$

$$= 2.852\sqrt{r_s m e^2/\kappa}$$

are obtained assuming straight lines $\vec{\mathbf{x}}(q)$ for simplicity. This yields upper bounds to the true values of $\mathcal{S}$ which may be reasonable particularly for $\mathcal{S}_{(123) \to (312)}$. The estimate for $\mathcal{S}_{(123) \to (213)}$ is surely worse because the classical path $\vec{\mathbf{x}}(q)$ is more difficult to estimate for the pair exchange. The chosen paths for both cases are indicated in Fig. 2. Thus the pair-exchange process (corresponding to the superexchange within the lattice description below) is slightly dominant compared to the ring process in the equilateral triangle. This supports a ground state of low total spin $S=1/2$. However, the triangle can easily be distorted so that $\mathcal{S}_{(123) \to (312)}$ is much reduced while $\mathcal{S}_{(123) \to (213)}$ remains almost unaffected, resulting in a crossover to a spin-polarized ground state[30,31] (see also below).

The existence of ring-exchange processes highlights a fundamental difference between a true lattice model and a continuum model. In order to accommodate such processes we need a better lattice approximation to the continuum than that suggested by the Wigner lattice. This may be achieved by introducing intermediate lattice points and corresponding localized one-electron orbitals. Orthogonalizing these one-electron orbitals then enables an orthonormal many-electron basis set to be constructed, as before. This is shown in Fig. 3 for the triangular dot in which an extra lattice point is inserted between each pair of vertices.

The low-energy eigenstates may now be expanded in this basis set. As before, the probability of occupation of the three vertices is highest, leading to a 2^3 equals eightfold degenerate ground manifold when the hopping terms are
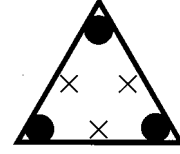

FIG. 3. Lattice points for the triangular quantum dot. In the ground manifold all three electrons will be close to the positions indicated by the circles. Excited (intermediate) states correspond to one or more electrons in localized orbitals centered on the crosses.

switched off. Higher-lying base states, corresponding to double occupation of a lattice site and to occupation of intermediate lattice sites may then be eliminated by degenerate perturbation theory, resulting once more in an effective spin Hamiltonian. Intermediate states which involve double occupation of a lattice site give rise to a Heisenberg superexchange term in the effective Hamiltonian, with $J = 8t^4/V^2U$, where t, V, and U have the same meanings as before but now refer to nearest-neighbor and on-site interactions for the new lattice. Longer-range interactions are ignored. [Note, however, that this is not necessary, it being straightforward to include longer-range interactions leading to a renormalization of J which will leave the form of the (Heisenberg) pair exchange unchanged.] There are two processes involved in this superexchange making equal contributions to J. These are shown in Fig. 4. These processes are analogous to superexchange in atomic systems in which the intermediate sites would correspond to ligand ions surrounding transition-metal ions. Recent examples of this kind of system are the copper-oxide planes of the high-temperature superconductors, for which there is a similar fourth-order expression for the superexchange.[32] It is also clear from this extended lattice description that other processes, which do not involve double occupation of a site (and therefore do not involve the exclusion principle), are potentially important. The lowest-order process of this type is also a pair exchange and occurs in fifth order. An example is shown in Fig. 4(b), which makes a contribution to J of order t^5/V^4. Despite being higher order
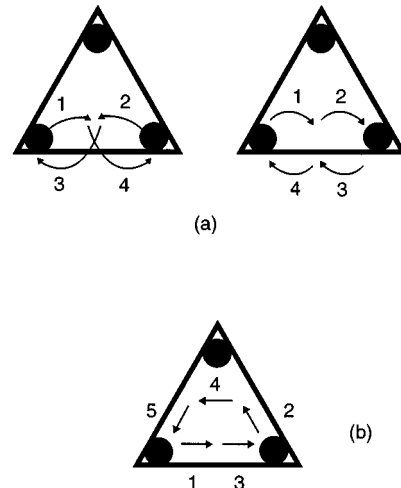

(a)

(b)

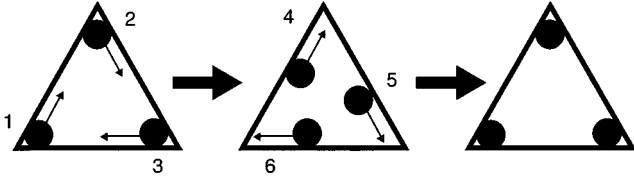FIG. 4. Superexchange processes. (a) Fourth order ($\sim t^4/V^2U$). (b) Fifth order ($\sim t^5/V^4$).

FIG. 5. A six-step ring process for three electrons in a triangular quantum dot. The electrons would move continuously and simultaneously in the direction of the arrows in the WKB approximation.

than the other superexchange terms, this process is, in fact, the largest since it does not involve double occupation of a site (i.e., there is no U factor in the energy denominator).

With intermediate lattice points it is easy to see that there are ring processes giving rise to simultaneous rotation of all three electrons. One such process, in which the three electrons are rotated cyclically by $2\pi/3$, is shown in Fig. 5. The process resembles the classical path which would contribute to the WKB tunneling rate, cf. Fig. 2. The former is a sixth-order process giving rise to a cyclic rotation operator in the effective Hamiltonian with amplitude $t^6/12V^5$. Summing over all such processes results directly in an effective ''ring'' operator, $-K(R_{2\pi/3}+R_{-2\pi/3})$, where K is a constant energy and $R_{2\pi/3}(R_{-2\pi/3})$ is an operator which performs a cyclic (anticyclic) rotation of all three electrons [cf. (3.22)]. We note that these rotation operators may be written as spin operators using the identities

$$R_{2\pi/3}\equiv P_{12}P_{23} \text{ and } R_{-2\pi/3}\equiv P_{23}P_{12}, \qquad (4.1)$$

where $P_{ij}\equiv 2\mathbf{s}_1\cdot\mathbf{s}_2+1/2$ is the Dirac exchange operator. Hence the effective spin Hamiltonian for three electrons in an equilateral triangular potential well becomes

$$H_{\text{eff}}=\frac{J}{2}\left[(P_{12}-1)+(P_{23}-1)+(P_{31}-1)\right]$$

$$-K(P_{12}P_{23}+P_{23}P_{12}). \qquad (4.2)$$

We see immediately from this form that the spin-polarized state has eigenenergy $-2K$. It is straightforward to complete the diagonalization of H_{eff} which results in a further pair of degenerate doublets at energy $K-3J/2$. Thus we see that the ring and exchange terms oppose each other with the former favoring a high-spin ground state and the latter a low-spin ground state. The crossover occurs at $J=2K$, which is not quite reached for the equilateral triangle, as discussed above within the WKB approximation..

This will not always be so for other geometries as follows immediately from the fact that we can change the shape of the dot in such a way that the ring processes are increased in amplitude relative to the exchange processes. An ''extreme'' example of this is the circular dot for which there is no barrier to the simultaneous rotation of the three electrons and the ground state should be spin polarized. The transition from high-spin to low-spin ground states in rings with increasing impurity barrier has been discussed recently[31] in the context of persistent currents.

With the inclusion of higher-order exchange processes involving also more than two particles, this completes the mapping of formerly continuous electron problems (2.1)

TABLE I. Analytical values for the fine-structure spectrum $E_m^{(N)}$ of N interacting electrons in a one-dimensional hard wall box within PSA for $N\leq 4$. S is the total spin of N fermions with $s=1/2$. The excitation energies $E_m^{(N)}-E_{\text{ground state}}^{(N)}$ are given in units of $J^{(N)}$.

N	S	$E_m^{(N)}-E_{\text{ground state}}^{(N)}$
2	0	0
2	1	$J^{(2)}$
3	1/2	0
3	1/2	$J^{(3)}$
3	3/2	$(3/2)J^{(3)}$
4	0	0
4	1	$(1+\sqrt{3}-\sqrt{2})J^{(4)}/2$
4	1	$(1+\sqrt{3})J^{(4)}/2$
4	0	$(2\sqrt{3})J^{(4)}/2$
4	1	$(1+\sqrt{3}+\sqrt{2})J^{(4)}/2$
4	2	$(3+\sqrt{3})J^{(4)}/2$

onto lattice models (3.18) for their low-energy and corresponding spin properties. This incorporates all permutational processes which according to the pocket-state description may be relevant. The above derivation of an effective-spin model for a triangular dot, including ring terms, is easily generalized to arbitrary shapes by inspecting all possible classes of ring and exchange terms on a suitably dense lattice into (3.18). The relative amplitudes of the various processes can be estimated semiclassically.

V. COMPARISON WITH EXACT RESULTS AND OTHER APPROXIMATIONS

To corroborate the lattice description for the low-energy and corresponding spin properties of quantum dots we compare the results from (3.18) with results obtained by numerically exact diagonalizations[14] and by the pocket-state method.[15]

The simplest model for an artificial atom is a hard wall box in one dimension. Rigorous properties for the sequence of spin states

$$E(S)<E(S') \qquad (5.1)$$

for $S<S'$ are known by a theorem of Lieb and Mattis.[33] $E(S)$ denotes the lowest energy of N almost arbitrarily interacting electrons to given spin

$$S=\begin{Bmatrix} 0 \\ 1/2 \end{Bmatrix},\ldots,N/2.$$

In particular, the ground-state spin must be minimal. This rule (5.1) is in obvious agreement with the description in terms of an antiferromagnetic Heisenberg (spin-1/2) chain (3.20), valid for this case according to Sec. III, where the exchange of adjacent electrons is the relevant permutational process and there is only one classical minimum-energy configuration, ($\nu=1$). In Table I the energy values of $N=2,3,4$ electrons are given in units of J as obtained within the pocket-state approximation (PSA), assuming $J_{12}=J_{23}=J_{34}$. These spectra agree exactly with the eigenvalues of the Heisenberg chain of $N=2,3,4$ spins apart from unimportant additive constants. Similarly, Fig. 6 shows the excitation energies for $N=3,\ldots,6$ and includes also results obtained by
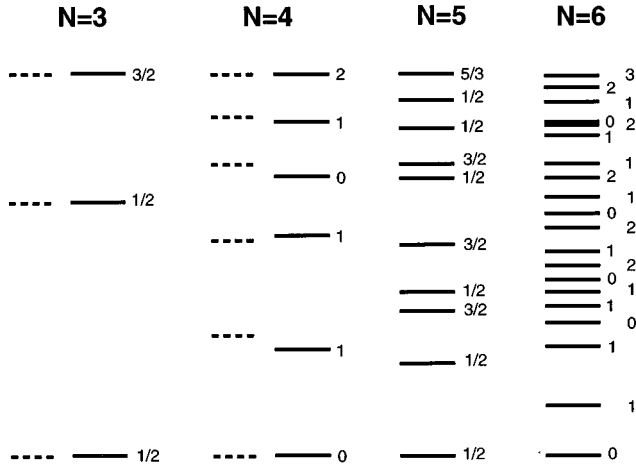
FIG. 6. Fine-structure multiplets of a quasi-one-dimensional quantum dot for $N=3,...,6$ as obtained directly from the pocket-state approximation and in exact agreement with the eigensolutions of the effective spin Hamiltonian. The dashed lines were obtained by direct numerical diagonalization of the interacting electron problem. The N dependence of $J^{(N)}$ is not considered and J has been adjusted to normalize the ''bandwidth'' of the multiplets.

numerical diagonalization of the Hamiltonian matrices for $N=3,4$ (dashed). For the cases $N=5$ and $N=6$ we also checked, by numerical diagonalization, that the Heisenberg chain shows exactly the same spectrum.

As a further example we investigated $N=2,...,5$ electrons in a two-dimensional square with hard walls. For these cases the interaction must be long range $w(|\mathbf{x}|) \sim |x|^{-\gamma}$ with $\gamma < 2$ in order to make the PSA applicable. The spectra obtained within PSA are shown in Fig. 7. For $N=4$ the nearest-

neighbor pair-exchange process has been compared with the competing process of all four electrons rotating cyclically by $\pi/4$,[15] in a similar way as it has been done for $N=3$ electrons in a triangle in the preceding section, with the result of the former being slightly dominant. In all cases the equilibrium positions of the electrons have been taken as sites for single-electron states for the lattice description, as discussed in Sec. III, and the importance of transition processes has been estimated semiclassically. For $N=5$ one electron is, by electrostatics, located in the center of the square being coupled antiferromagnetically, according to (3.20), to the four electrons placed in the corners. The Heisenberg model is appropriate since there is only one classical equilibrium configuration ($\nu=1$). Neglecting next-nearest-neighbor exchange results in an $S=3/2$ ground-state spin, using the PSA and permutation group theory. This result is immediately understandable from the Heisenberg spin Hamiltonian, which clearly has a quartet ground state. Furthermore, we have checked that for all spectra, the corresponding Heisenberg ($N=4,5$) or $t-J-V$ ($N=2,3$) Hamiltonians exactly reproduce the correct ordering of the spin multiplets and the correct energy splittings provided that the parameters t, J, and V are chosen to be consistent with the corresponding tunneling amplitudes in the PSA.

As a third example we look at the spectrum of three electrons in a one-dimensional ring. In Sec. IV we explained why the ground state is high spin ($S=3/2$), which is also found in the pocket-state description. Two degenerate low-spin ($S=1/2$) excited states are higher in energy by the rotational constant $h^2/2mNL^2$, where L is the circumference of the ring. They are additionally shifted by the magnitude of the pair-exchange process J towards lower energy, in agreement with (4.2).

VI. SUMMARY AND OUTLOOK

Based on the pocket-state description of the low-energy excitations in finite and *a priori* continuous systems of interacting electrons at low densities we have derived a lattice formulation for this problem. Nonorthogonal single-electron states centered near the positions where the electrons would be in the classical minimum-energy configurations are orthogonalized, leading to contributions from double occupancies $\sim U_i n_{i\uparrow} n_{i\downarrow}$ in an effective Hubbard model description. Subsequent elimination of high-energy states ($\sim U_i$ or $\sim V_{ij}$, from nearest-neighbor occupations) yields effective antiferromagnetic Heisenberg [Eq. (3.20) for $\nu=1$] or charge-spin Hamiltonians [Eq. (3.18) for $\nu>1$] depending on the number ν of classical minimum-energy configurations. An extended version of the Hubbard model must be considered if highly symmetric geometries or ring processes are important. A crucial enhancement has been to enable ''ring-exchange'' processes to be included, corresponding to the cyclic permutation of $N>2$ electrons. Intermediate lattice points were introduced and the additional states corresponding to their single occupation were also eliminated by higher-order perturbation theory, even though they are much lower in energy than states corresponding to double occupation. This yields generalized effective spin-1/2 models containing up to $(N-1)$-fold products of pairs of spin operators [see Eq. (4.1)]. The magnitudes of the parameters for the superexchanges J
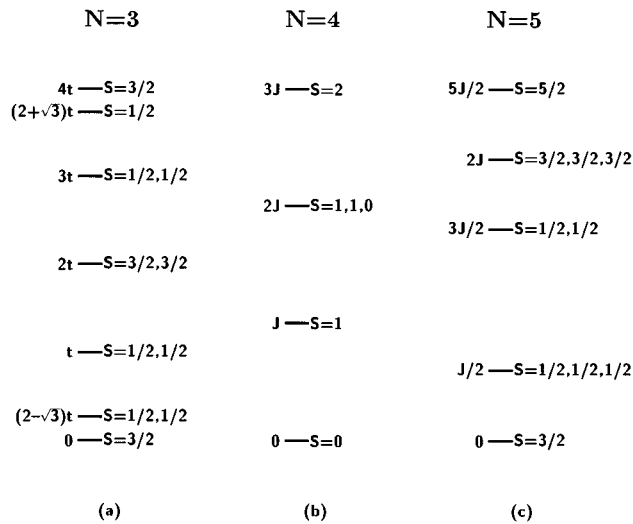

FIG. 7. Fine-structure spectra of (a) $N=3$, (b) $N=4$, and (c) $N=5$ electrons in a 2D square as obtained within the pocket-state approximation. In (a) the dominant tunneling process (t) corresponds to nearest-neighbor hopping of an electron whereas in (b) and (c) the dominant tunneling process is nearest-neighbor exchange (J). All spectra are identical with those obtained from the corresponding charge-spin Hamiltonian.

and the ring exchanges K can be estimated semiclassically.

Apart from providing a quantitative description of the low-energy spectra in quantum dots the mapping onto lattice models is, in itself, very illuminating. For example, in cases that can be mapped onto the antiferromagnetic Heisenberg model for the low-energy states, the spectrum consists of a level multiplet of ''band width'' NJ where J, the nearest-neighbor superexchange integral, depends exponentially on the mean electron distance r_s. The highest-energy state within this multiplet is the spin-polarized state, in agreement with what has been derived within the pocket-state approximation using less obvious arguments. All spectra obtained by the lattice descriptions coincide exactly with those found in the pocket-state[15] approximation and are in very convincing agreement with results gained by numerical diagonalizations.[14,34] The computational effort required for the former is, however, considerably less compared to both of the other methods. This will enable much larger systems with $N>20$ to be investigated.

In certain geometries of two-dimensional quantum dots, $\nu>1$ classical configurations of lowest electrostatic energy may exist, leading to an effective spin-charge model instead of a spin-only effective model. While such situations are straightforward to deal with by the lattice method, we should point out that in real experimental situations the high symmetry will be lowered by a polarizable environment for the following reason. The energetically most favorable locations for the quantum dot electrons depend on the distribution of surrounding (nonconducting) charges, which themselves are influenced by the distribution of the (Wigner localized but under transport conditions conducting) dot charges. Self-consistency allows the dot electrons to lower the total energy by adjusting their environment. For example, two electrons in a square will easily break the twofold symmetry of the classical ground states by polarizing their surroundings, leaving a diamond-shaped configuration for the potential. The interplay between the surroundings and the granular electron density of the dot finally tends to lower the number of classical low-energy configurations. Only configurations with energies smaller than the bandwidth $\sim NJ$ eventually need to be considered explicitly. This plays a particular role, e.g., in double-dot systems.[35] Additionally, one should keep in mind that the shape of the quantum dot also depends on voltages applied to side gates,[36] so that the fine-structure spectra may change with gate voltage.

The lattice description simplifies considerably the determination of excitations in quantum dots. These excited levels may be deduced implicitly from nonlinear transport experiments.[5] Furthermore, transport is qualitatively influenced by the total spins of the many-electron states by two types of *spin blockade*.[6,37]

The occurrence of a nonminimal total spin for the ground state in a finite electron system is a direct consequence of the geometry of the boundary. For systems which can be represented by an antiferromagnetic Heisenberg model, this relationship is obvious (cf. discussion of the square dot with $N=5$ in Sec. V). Apart from the electron number the spin values of ground and of excited states should depend very sensitively on the shape of the quantum dot. In future research this will be investigated systematically to allow specific suggestions for experimental design.

Another highly relevant topic for real experimental situations is to apply the mapping derived in the present work to study the interplay between mutual interactions of the quantum dot electrons and impurities. No reliable picture exists presently, which demonstrates our lack of understanding of the persistent currents observed in mesoscopic rings. Theory is still not capable of explaining even the order of magnitude of the high values found experimentally. It is known that one-dimensional models of rings are insufficient to describe this problem.[38] Furthermore, evidence exists that the electron spin is important.[39,31] Our mapping onto lattice models demonstrates that calculations based on the Hubbard model[40–42] are not significantly influenced by the lattice but indeed reproduce the low-energy properties of the original continuous problems in the presence of strong interactions correctly if the parameters, particularly the filling of the former, are interpreted accordingly. Advantage can be taken of the comparably large electron numbers that can be dealt with by our method, which would otherwise be intractable. This will allow the investigation of multiple channels in two-dimensional rings of finite widths in the presence of impurities and flux.

[1] D. V. Averin and K. K. Likharev, J. Low Temp. Phys. **62**, 345 (1986); *Single Charge Tunneling*, Vol. 294 of *NATO Advanced Study Institute, Series B: Physics*, edited by H. Grabert and M. Devoret (Plenum Press, New York, 1992), and references therein; Single Charge Tunneling, edited by H. Grabert, special issue of Z. Phys. B **85**, 317 (1991).

[2] Ch. Sikorski and U. Merkt, Phys. Rev. Lett. **62** 2164, (1989).

[3] B. Meurer, D. Heitmann, and K. Ploog, Phys. Rev. Lett. **68**, 1371 (1992); D. Heitmann and J. P. Kotthaus, Phys. Today **56**, (6), 56 (1993).

[4] U. Meirav, M. A. Kastner, and S. J. Wind, Phys. Rev. Lett. **65**, 771 (1990).

[5] D. V. Averin and A. N. Korotkov, J. Low Temp. Phys. **80**, 173 (1990); A. T. Johnson, L. P. Kouwenhoven, W. de Jong, N. C. van der Vaart, C. J. P. M. Harmanns, and C. T. Foxon, Phys. Rev. Lett. **69**, 1592 (1992); J. Weis, R. J. Haug, K. v. Klitzing, and K. Ploog, *ibid*. **71**, 4019 (1993); E. B. Foxman, P. L. McEuen, U. Meirav, N. S. Wingreen, Y. Meir, P. A. Belk, N. R. Belk, M. A. Kastner, and S. J. Wind, Phys. Rev. B **47**, 10020 (1993).

[6] D. Weinmann, W. Häusler, W. Pfaff, B. Kramer, and U. Weiss, Europhys. Lett. **26**, 689 (1994); W. Pfaff, D. Weinmann, W. Häusler, B. Kramer, and U. Weiss, Z. Phys. B **96**, 201 (1994).

[7] C. Bruder and H. Schoeller, Phys. Rev. Lett. **72**, 1076 (1994); L.

P. Kouwenhoven, S. Jauhar, K. McCormick, D. Dixon, P. L. McEuen, Yu. V. Nazarov, N. C. van der Vaart, and C. T. Foxon, Phys. Rev. B **50**, 2019 (1994).

[8] U. Merkt, Physica B **189**, 165 (1993).

[9] A. V. Chaplik, Pis'ma Zh. Eksp. Teor. Fiz. **52**, 681 (1990) [JETP Lett. **52**, 31 (1990)].

[10] M. Wagner, A. V. Chaplik, and U. Merkt, Phys. Rev. B **51**, 13817 (1995).

[11] M. A. Kastner, Rev. Mod. Phys. **64**, 849 (1992).

[12] D. Pfannkuche, V. Gudmundsson, and P. A. Maksym, Phys. Rev. B **47**, 2244 (1993).

[13] P. A. Maksym and T. Chakraborty, Phys. Rev. Lett. **65**, 108 (1990); U. Merkt, J. Huser, and M. Wagner, Phys. Rev. B **43**, 7320 (1991); D. Pfannkuche and R. R. Gerhards, *ibid.* **44**, 13132 (1991); W. Häusler, B. Kramer, and J. Mašek, Z. Phys. B **85**, 435 (1991); P. Hawrylak and D. Pfannkuche, Phys. Rev. Lett. **70**, 485 (1993).

[14] W. Häusler and B. Kramer, Phys. Rev. B **47**, 16353 (1993).

[15] W. Häusler, Festkörperprobleme/Adv. Solid State Phys. **34**, 171 (1994); Z. Phys. B **99**, 551 (1996).

[16] K. A. Chao, J. Spalek, and A. M. Oles, Phys. Rev. B **18**, 3453 (1978).

[17] J. H. Jefferson, J. Phys. C **21**, 1193 (1988).

[18] D. E. Rutherford, *Substitutional Analysis* (The Edinburgh University Press, London, 1948); M. Hamermesh, *Group Theory and its Applications to Physical Problems* (Addison-Wesley, Reading, MA, 1962); new edition by (Dover Publications, New York, 1989).

[19] J. Hubbard, Proc. R. Soc. London Ser. A **276**, 238 (1963).

[20] E. P. Wigner, Phys. Rev. **46**, 1002 (1934).

[21] E. Dagotto, Rev. Mod. Phys. **66**, 763 (1994).

[22] K. Jauregui, W. Häusler, and B. Kramer, Europhys. Lett. **24**, 581 (1993).

[23] A. Hüller, Z. Phys. B **36**, 215 (1980).

[24] P. O. Löwdin, J. Chem. Phys. **18**, 365 (1950).

[25] I. Lindgren, J. Phys. B **7**, 2441 (1974).

[26] J. R. Schrieffer and P. A. Wolff, Phys. Rev. **149**, 491 (1966).

[27] It is possible to include the V term in the unperturbed Hamiltonian. However, this introduces complications in the perturbation expansions (since the intermediate-state energies depend on their environment) which are best avoided. Since we are interested in the regime for which $U \gg V$, including V in the perturbation introduces only a small error.

[28] L. F. Feiner, J. H. Jefferson, and R. Raimondi, Phys. Rev. B **51**, 12797 (1995).

[29] F. C. Zhang and T. M. Rice, Phys. Rev. B **37**, 3757 (1988); J. H. Jefferson, Physica B **165-166**, 1013 (1990); J. H. Jefferson, H. Eskes, and L. F. Feiner, Phys. Rev. B **45**, 7959 (1992); H.-B. Schüttler and A. J. Fedro, Phys. Rev. B **45**, 7588 (1992); C. D. Batista and A. A. Aligia, *ibid.* **47**, 8929 (1993); V. I. Belinicher, A. L. Chernyshev, and L. V. Popovich, *ibid.* **50**, 13768 (1994); L. F. Feiner, J. H. Jefferson, and R. Raimondi, Phys. Rev. B **53**, 8751 (1996); R. Raimondi, J. H. Jefferson, and L. F. Feiner, *ibid.* **53**, 8774 (1996).

[30] K. W. H. Stevens, J. Phys. C **16**, 5765 (1983).

[31] W. Häusler and B. Kramer, in *Quantum Dynamics of Submicron Structures*, Vol. 291 of *NATO Advanced Study Institute, Series E: Applied Sciences*, edited by H. A. Cerdeira, B. Kramer, and G. Schön (Kluwer, Dordrecht, 1995); W. Häusler, Physica B **222**, 43 (1996).

[32] H. Eskes and J. H. Jefferson, Phys. Rev. B **48**, 9788 (1993).

[33] E. Lieb and D. Mattis, Phys. Rev. **125**, 164 (1962).

[34] G. W. Bryant, Phys. Rev. Lett. **59**, 1140 (1987).

[35] N. C. van der Vaart, S. F. Godijn, Yu. V. Nazarov, C. J. P. M. Harmans, J. E. Mooij, L. W. Molenkamp, and C. T. Foxon, Phys. Rev. Lett. **74**, 4702 (1995); F. Hofmann, T. Heinzel, D. A. Wharam, J. P. Kotthaus, G. Böhm, W. Klein, G. Tränkle, and G. Weimann, Phys. Rev. B **51**, 13872 (1995); R. H. Blick, R. J. Haug, J. Weis, D. Pfannkuche, K. v. Klitzing, and K. Eberl, *ibid.* **53**, 7899 (1996).

[36] L. P. Kouwenhoven, Ph.D. thesis, Technical University of Delft, 1992.

[37] D. Weinmann, W. Häusler, and B. Kramer, Phys. Rev. Lett. **74**, 984 (1995).

[38] R. Berkovits and Y. Avishai, Europhys. Lett. **29**, 475 (1995).

[39] T. Giamarchi and B. S. Shastry, Phys. Rev. B **52**, 14809 (1995).

[40] N. Yu and M. Fowler, Phys. Rev. B **45**, 11795 (1992).

[41] M. Ramin, B. Reulet, and H. Bouchiat, Phys. Rev. B **51**, 5582 (1995).

[42] R. Römer, A. Punnoose, Phys. Rev. B **52**, 14809 (1995).